Biochimica et Biophysica Acta 1787 (2009) 168–175

Contents lists available at ScienceDirect

Biochimica et Biophysica Acta

journal homepage: www.elsevier.com/locate/bbabio

Triplet–triplet energy transfer in Peridinin-Chlorophyll *a*-protein reconstituted with Chl *a* and Chl *d* as revealed by optically detected magnetic resonance and pulse EPR: Comparison with the native PCP complex from *Amphidinium carterae*

Marilena Di Valentin [a], Giancarlo Agostini [c], Enrico Salvadori [a], Stefano Ceola [a], Giorgio Mario Giacometti [b], Roger G. Hiller [d], Donatella Carbonera [a,*]

[a] *Dipartimento di Scienze Chimiche, Università di Padova, via Marzolo 1, 35131 Padova, Italy*
[b] *Dipartimento di Biologia, Università di Padova, vi U. Bassi, 35131 Padova, Italy*
[c] *CNR, Istituto di Chimica Biomolecolare, Sezione di Padova, via Marzolo 1, 35131 Padova, Italy*
[d] *Department of Biological Sciences, Macquarie University, 2109 NSW, Australia*

ARTICLE INFO

Article history:
Received 16 October 2008
Received in revised form 11 December 2008
Accepted 12 December 2008
Available online 24 December 2008

Keywords:
PCP
Peridinin
Carotenoid
Triplet
ODMR
EPR

ABSTRACT

The triplet state of the carotenoid peridinin, populated by triplet–triplet energy transfer from photoexcited chlorophyll triplet state, in the reconstituted Peridinin-Chlorophyll a-protein, has been investigated by ODMR (Optically detected magnetic resonance), and pulse EPR spectroscopies. The properties of peridinins associated with the triplet state formation in complexes reconstituted with Chl *a* and Chl *d* have been compared to those of the main-form peridinin-chlorophyll protein (MFPCP) isolated from *Amphidinium carterae*. In the reconstituted samples no signals due to the presence of chlorophyll triplet states have been detected, during either steady state illumination or laser-pulse excitation. This demonstrates that reconstituted complexes conserve total quenching of chlorophyll triplet states, despite the biochemical treatment and reconstitution with the non-native Chl *d* pigment. Zero field splitting parameters of the peridinin triplet states are the same in the two reconstituted samples and slightly smaller than in native MFPCP. Analysis of the initial polarization of the photoinduced Electron-Spin-Echo detected spectra and their time evolution, shows that, in the reconstituted complexes, the triplet state is probably localized on the same peridinin as in native MFPCP although, when Chl *d* replaces Chl *a*, a local rearrangement of the pigments is likely to occur. Substitution of Chl *d* for Chl *a* identifies previously unassigned bands at ~ 620 and ~ 640 nm in the Triplet-minus-Singlet (T−S) spectrum of PCP detected at cryogenic temperature, as belonging to peridinin.

1. Introduction

Dinoflagellates belong to the group of marine eukaryotic algae which possess two different light harvesting complexes, an intrinsic membrane bound LHC, and the water soluble peridinin–chlorophyll-a protein (PCP) which contains only peridinin and Chl *a*.

Depending on the species, the PCP complex consists of either an apoprotein of 32 kDa binding 8 peridinin and 2 Chl *a* molecules, or is a dimer of 15 kDa monomers each binding 4 peridinins and 1 Chl *a* [1]. The amino acid sequence of the 32 kDa protein form indicates that it arose by a gene duplication and fusion as it consists of two parts with 56% identity and joined by a spacer region. Moreover, the 15 kDa PCP of *Heterocapsa pygmaea* also has high homology with both domains of the 32 kDa species [1].

The X-ray structure of the main form of PCP (MFPCP) from *A. carterae* has been resolved to 2.0 Å [2]. The basic structure is a trimer. In each subunit of the trimer the pigments are arranged as two pseudo-identical domains of 4 peridinins, and a Chl *a* molecule, as shown in Fig. 1. The pigments are located in the hydrophobic cavity formed by the protein. The peptide primary sequences of the -N and -C terminal regions form structurally almost identical domains, each consisting of eight alpha-helices. Recently, the X-ray structure of high-salt PCP (HSPCP), which has a molecular weight of 34 kDa, has also been determined (T. Schulte, F.P. Sharples, R.G. Hiller, E. Hofmann, coordinates have been deposited in the Brookhaven Protein Data Bank under ID 2C9E, unpublished) [3]. It shows considerable similarity with the MFPCP structure in terms of pigment arrangement, except for the absence of two symmetry related peridinins, called PID612/PID622 in MFPCP [2].

PCP has been extensively investigated with many different spectroscopic techniques as well as by theoretical studies, in order

Abbreviations: PID, peridinin; Chl, chlorophyll; PCP, peridinin-chlorophyll protein; *A. carterae*, *Amphidinium carterae*; MFPCP, main form PCP; ODMR, optically detected magnetic resonance; FDMR, fluorescence detected magnetic resonance; ADMR, absorption detected magnetic resonance; ZFS, zero field splitting; ISC, intersystem crossing; ESE, electron spin echo

* Corresponding author. Tel.:+39 049 827 5144; fax: +39 049 827 5161.
E-mail address: donatella.carbonera@unipd.it (D. Carbonera).

0005-2728/$ – see front matter © 2008 Elsevier B.V. All rights reserved.
doi:10.1016/j.bbabio.2008.12.004

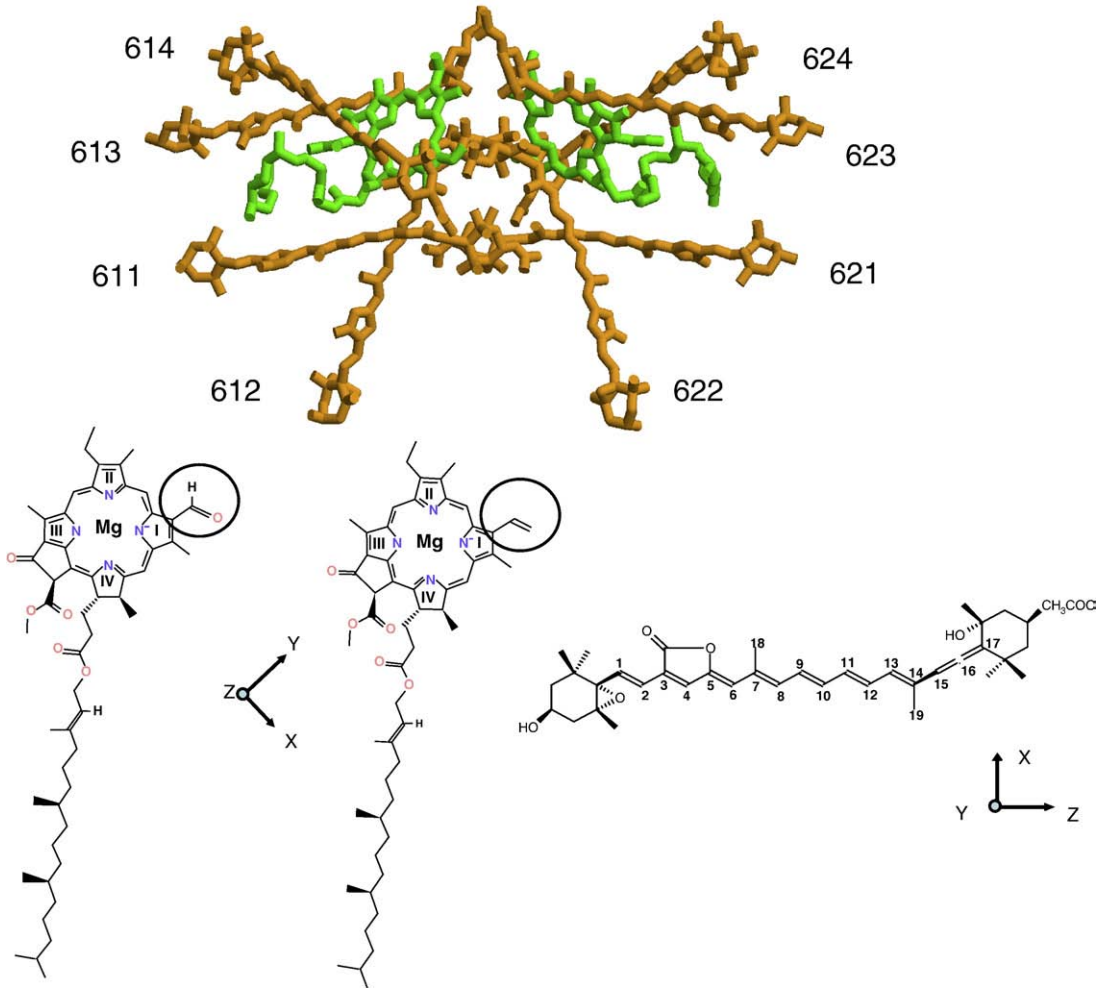

Fig. 1. (Top) Structure of the pigments associated with the monomeric basic unit of the PCP complex from *A. carterae*. Structure taken from coordinates of MFPCP complex 1PPR deposited in the Brookhaven Protein Data Bank. The numbers refer to the peridinins in the PDB files (Bottom) Molecular structure of Chl *d* (left) and Chl *a* (right) and peridinin with the orientation of the ZFS tensor axes.

to correlate the spectroscopic properties with the arrangement of the pigments in the protein, as resolved by the X-ray structure [4–9]. More recently, reconstitution of functional PCP from heterologously-expressed apoprotein mixed with pigments extracted from native PCP, has been obtained [10]. Constructs of full-length, and also N-terminal domain alone PCP (N-PCP), have been produced and reconstituted in vitro with both native and altered pigment composition. The N-PCP is a 16 kDa protein which corresponds to the "half-mer" of the monomeric PCP from *A. carterae*. When the unfolded N-PCP is reconstituted with the same pigments as those present in native PCP, the protein forms a 32 kDa homo-dimer [10–12]. The Circular Dichroism, absorption, fluorescence and florescence excitation spectra, have shown that the reconstituted samples are characterized by spectroscopic properties very similar to those of the native samples [5,10].

The genetic and biochemical manipulations of PCP have opened the way to a better understanding of the energy transfer between peridinins and Chls. [13,16]. It has been shown that the substitution of Chl *a* by Chl *b*, Chl *d*, acetyl-Chl *a* and BChl *a* does not alter significantly the singlet energy transfer pathway and its efficiency. The minor differences observed have been rationalized in terms of specific effects due to diverse spectral overlaps between the pigments [13,15]. Experimental results on hetero-chlorophyllous N-PCP complexes, obtained by adding mixture of different Chls during the reconstitution process, indicate specific binding affinities in the protein [12,13,14].

In addition to their main light harvesting function, peridinin molecules in PCP also play a photo-protective role [17–19]. The low-lying triplet state of peridinin is capable of trapping Chl *a* triplet states, avoiding the formation of potentially harmful singlet oxygen. In MFPCP the lifetime of the Chl *a* triplet state is of the order of 20 ns; within this time a triplet state is formed on the peridinins and decays through radiationless intersystem crossing channels with a lifetime of 10 μsec at room temperature [19].

In MFPCP, HSPCP and also in N-PCP reconstituted with the native pigments, the triplet-triplet energy transfer takes place with 100% efficiency [5,20–23]. To study the formation of triplet state in native PCP complexes, we have used in the past different spectroscopic techniques: ODMR (optically detected magnetic resonance), to correlate the magnetic properties of the triplet state with the optical properties of the system [18,21,24–25]; time-resolved EPR (TR-EPR) [20–21] to identify the peridinin-chlorophyll pairs directly involved in the triplet energy transfer, and pulse-ENDOR for insights into the electronic structure of the peridinin triplet state [21,23]. By comparing the TR-EPR spectra of MFPCP and HSPCP and their X-ray structures, we suggested that the pathway of triplet quenching and triplet localization was very similar in the two complexes [21]. We also performed pulse-EPR and pulse-ENDOR experiments on MFPCP and HSPCP. The ENDOR investigation, accompanied by DFT calculation of the hyperfine couplings strongly supported the hypothesis of localization of the triplet state on one peridinin in each subcluster of both MFPCP and HSPCP complexes [21,23]. The triplet state of

peridinins in N-PCP has not been characterized to the same extent although a pulse-ENDOR experiment on the triplet state of the Chl *a* N-PCP has been reported [22].

In this work we compare the properties of peridinin triplet states, populated by triplet –triplet energy transfer from photoexcited chlorophyll triplet state, in complexes reconstituted with Chl *a* with those previously reported for peridinins involved in triplet state population in the native MFPCP from *A. carterae*. We also extend the study to Chl *d* N-PCP to explore the effect of the structure of the Chl on the properties of the triplet-triplet energy transfer process. Chl *d* has a Q_y band at 700 nm, red-shifted compared to the Chl *a* Q_y band (670 nm). A splitting of the Soret and Qy bands observed in Chl *a* N-PCP, but not in Chl *d* N-PCP complexes, has been suggested to be due to the different configurations that the vinyl group in Ring I can adopt (see Fig. 1). In contrast the carbonyl group in Ring I of Chl *d* may adopt only a single configuration [4]. Moreover, while the Chl-protein interaction induces a blue-shift of the Q_y band in the low temperature spectra of Chl *a*, Chl *b*, and 3-Acetyl-Chl *a*, compared to the spectra taken in 2-MTHF at low temperature, no shift is observed for Chl *d* [4].

The efficiency of the triplet-triplet transfer depends strictly on the relative geometry of the donor and the acceptor and requires optimization in terms of wavefunction overlap and pigment interactions. In this work we try to rationalize the effect induced by the insertion of Chl *d* on the triplet quenching mechanism occurring in PCP. The results are compared to those previously obtained for native MFPCP and discussed in terms of energy transfer properties, specific pathway for triplet quenching and protein structure.

2. Materials and methods

2.1. Sample preparation

Reconstitution of N-PCP complexes from heterologously expressed N-Domain PCP apoprotein was as described previously [10]. Samples of purified reconstructed PCP were stored in aliquots at −70 °C and diluted with buffer immediately prior to use. Absorbance at the Chl Qy band was 0.8 for the ODMR experiments and about 2.0 times for EPR experiments. Pigments for reconstituting Chl *a* N-PCP were extracted from MFPCP and Chl *d* was extracted from cells of *Acaryochloris marina* by the procedure of Martinson and Plumley and purified by reverse phase HPLC [26].

2.2. Spectroscopic methods

2.2.1. ODMR experiments

60% v/v glycerol was added to the samples in order to obtain a transparent glass upon cooling of the sample to 1.8 K. At cryogenic temperatures spin-lattice relaxation is inhibited and the ODMR signal is intense. Fluorescence and Absorption detected magnetic resonance (FDMR, ADMR) experiments were performed in a home built apparatus, previously described in detail [27–28]. ODMR is a double resonance technique based on the simple principle that, when a triplet steady state population is generated upon illumination, the application of a resonant microwave electromagnetic field between two spin sublevels of the triplet state, generally induces a change of the steady state population of the triplet state itself, due to the anisotropy of the decay and population rates of the three spin sublevels. The induced change of the triplet population may be detected as a corresponding change of the emission and/or absorption of the system [24–25]. Amplitude modulation of the applied microwave field (on–off) is used to increase the S/N ratio by means of a phase sensitive lock-in amplifier (EG&G 5220) detection.

In the FDMR experiments the fluorescence, excited by a halogen lamp (250 W) focused into the sample and filtered by a broadband 5 cm solution of $CuSO_4$ 1 M, was collected at 45 °C through appropriate band-pass filters (10 nm FWHM) by a silicon photodiode (Centronic OSI 5) before entering the lock-in amplifier. Low temperature emission spectra were detected in the same apparatus used for ODMR experiments, using the same excitation source, but substituting the band-pass filters before the photodiode by a monochromator (Jobin Yvon HR250, 3 nm/mm dispersion).

In the absorption detection mode (ADMR) the sample is excited by a halogen lamp (250 W) focused into the sample and filtered by 5 cm water and heat filters. The transmitted light, modulated by the on–off of the microwave field, after passing a monochromator, is detected by a photodiode and the signal is finally amplified and demodulated in the lock-in amplifier.

By fixing the microwave frequency at a resonant value while sweeping the detection wavelength, microwave-induced Triplet-minus-Singlet (T−S) spectra can be registered.

2.2.2. Pulse EPR experiments

Oxygen was removed from the samples by flushing argon in the EPR capillary before freezing. Glycerol, previously degassed by several cycles of freezing and pumping, was added (60%v/v) to obtain a transparent matrix.

Experiments were performed on a Bruker Elexsys E580 pulsed EPR spectrometer. Laser excitation at 532 nm (10 mJ per pulse and repetition rate of 10 Hz) was provided by the second harmonic of a Nd:YAG laser (Quantel Brilliant) in a dielectric cavity. The temperature was controlled with a Helium cryostat (Oxford CF935) driven by a temperature controller (Oxford ITC503).

Field-swept ESE spectra were recorded using a 2-pulse ESE sequence according to the scheme: flash-DAF-π/2-τ-π-τ-echo (DAF = delay after laser flash); the value of DAF was fixed at 50 ns. ESE-detected kinetics at the triplet canonical orientations were recorded using a 2-pulse (flash-DAF-π/2-τ-π-τ-echo) ESE sequence after a variable DAF between the laser flash and the first MW pulse. The π/2-pulse was of 16 ns and the delay τ was set at 200 ns for the field-swept ESE experiment and to 120 ns for the ESE-detected kinetics.

2.3. EPR spectral analysis

Calculation of the sublevel triplet state populations of the acceptor starting from those of the donor has been performed using a home-written program in Mathematica® software following the formalism of ref. [20–21] in the limit of a triplet-triplet energy transfer which is fast, compared to the time evolution of the donor triplet spectrum and is slow enough to allow spin alignment in the external magnetic field. Simulations of the powder spin polarised triplet spectra were performed using a program written in MatLab® with the aid of the Easyspin routine (ver. 2.6.0) [29]. The program is based on the full diagonalization of the triplet state spin Hamiltonian, taking into account the Zeeman and magnetic dipole-dipole interactions, assuming a powder distribution of molecular orientations with respect to the magnetic field direction.

Simulations of the DAF kinetics were performed according to the method previously described in ref. [20].

3. Results

The absorption spectra of the reconstituted samples, taken at room temperature, are identical to those reported by Ilagan et al. 2006 [4]. At 1.8 K the fluorescence emission maximum is at 672 nm, for Chl *a* N-PCP, and 700 nm for Chl *d* N-PCP, values in agreement with those reported for the emission at 77 K [4].

3.1. ODMR

Steady state illumination of PCP at cryogenic temperatures leads to the formation of peridinin triplet states, which can be detected by monitoring the change of the Chl emission induced by a microwave field swept in the spectral region where carotenoid triplet states are

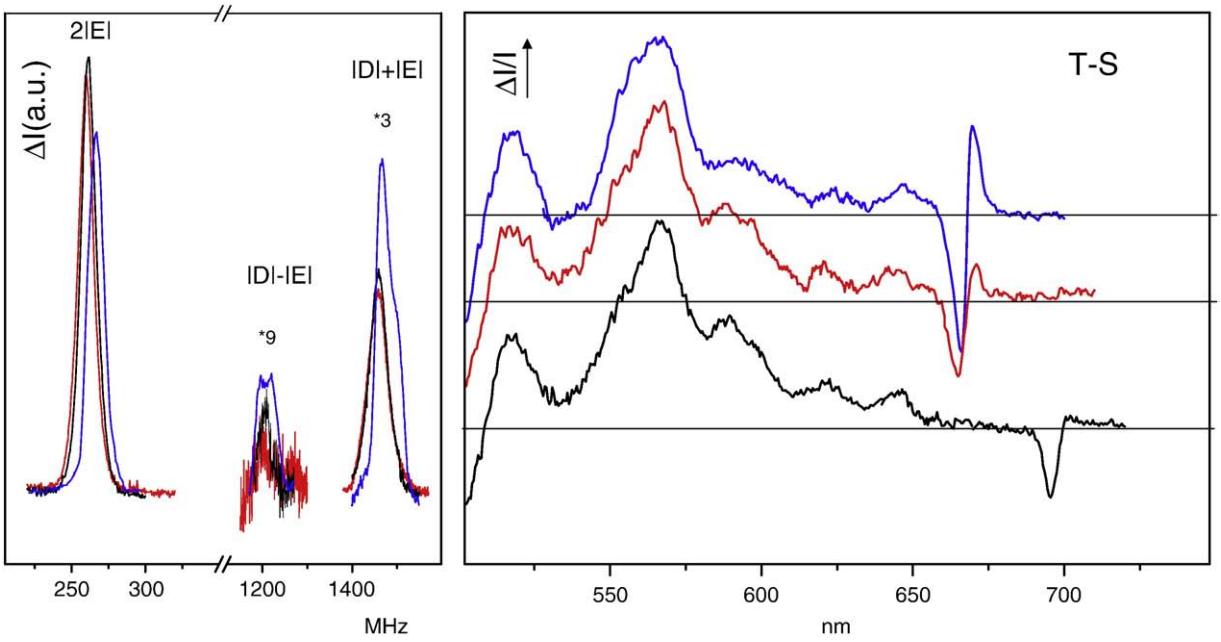

Fig. 2. (Left) FDMR spectra of peridinin triplet state in Chl *a* N-PCP (red), Chl *d* N-PCP (black) and MFPCP (blue) at 1.8 K. MFPCP curves from [18]. Detection wavelength: 670 nm for Chl *a* N-PCP, 700 nm for Chl *d* N-PCP; mod. freq. 323 Hz, Mw power 1 W, 10 scans. (Right) T−S spectra of Chl *a* N-PCP (red), Chl *d* N-PCP (black) detected at the maximum of 2|E| transition. T−S spectrum of MFPCP (blue) from [34]. Spectra have been rescaled for better comparison. The lines corresponding to ΔI/I = 0 are shown. Modulation frequency: 323 Hz, Microwave power: 1 W, T = 1.8 K. ΔI/I ≅ ΔA.

expected to show resonant transitions between pairs of spin sublevels [18,27,30–32].

FDMR spectra of Chl *a* N-PCP and Chl *d* N-PCP, in the microwave field region where the 2|E|, the |D|−|E| and the |D|+|E| transitions of peridinins are expected, are shown in Fig. 2 (left).

Three transitions, characterized by the polarization pattern usually found for carotenoids (intensity of 2|E| ≫ |D|+|E| > |D|−|E|), have been detected at 261, 1206, 1460 MHz for Chl *d* N-PCP and 260, 1202, 1460 MHz for Chl *a* N-PCP giving essentially the same ZFS parameters (D| = 0.0443 ± 0.0001 cm^{-1} |E| = 0.0043 ± 0.0005 cm^{-1}). The transition frequencies are slightly shifted with respect to those previously reported for native MFPCP (i.e. 267, 1203(sh1229), 1465 (sh1499) MHz) [18,33–34]. The |D|+|E| and |D|−|E| transitions are largely inhomogeneous for both the N-PCP complexes but lack the two well-resolved components present in native MFPCP (D| = 0.0448 cm^{-1}, |E| = 0.0044 cm^{-1} and |D| = 0.04586 cm^{-1}, |E| = 0.0045 cm^{-1}).

In both reconstituted samples, as in native MFPCP [18,20,34], no signals which could be ascribed to the presence of unquenched Chl *a* triplet states have been detected under steady state illumination.

The microwave-induced T−S spectra, taken by fixing the microwave frequency at the maximum of the intense 2|E| transition (260–261 MHz), are shown in Fig. 2 (right). The T−S spectra of Chl *a* N-PCP is very similar to that, previously reported, for native MFPCP (shown also in Fig. 2, from [34]) and is almost identical to the spectrum of Chl *d* N-PCP in the range from 450 to 650 nm. The main difference between the two reconstituted samples is in the spectral position, and relative intensity, of the bleaching corresponding to the Q_y band of Chl (665 nm for Chl *a* N-PCP vs 695 nm for Chl *d* N-PCP). The bleaching is accompanied at longer wavelength by a small positive band which is more pronounced in Chl *a* N-PCP than in Chl *d* N-PCP.

3.2. Pulse EPR

We have previously shown that, in the case of carotenoid triplet state, kinetic measurements in time-resolved EPR are hampered by the presence of microwave-induced transition probability effects. Pulse EPR is more appropriate, because it does not suffer from the above complication as there is no microwave field present in the period between the photo-generation of the triplet state and its detection [23]. The kinetics of population and decay of the triplet spin sublevels, obtained by monitoring the echo intensity as a function of DAF, at the low-field canonical orientations of the ZFS tensor (Z^-,Y^+,X^+), are shown in Fig. 3 together with the ESE-detected spectrum at a DAF of 50 ns, at 20 K.

Due to the absence of fast and anisotropic relaxation processes depending on the orientation of the triplet state with respect to the magnetic field, the ESE detected spectra taken at early times after the laser flash are substantially the same, in terms of shape, as the initial TR-EPR spectra (data not shown), as already observed for native MFPCP. No signals which could be ascribed to the presence of unquenched Chl triplet states have been detected in either TR-EPR or ESE detected spectra at early and late times after the laser flash in the two reconstituted samples, in agreement with the ODMR results. Direct comparison of the ESE-detected spectra and decay curves, with the corresponding data on native MFPCP taken from ref [23] are reported in Fig. 3.

Simulations of the ESE-detected spectra and ESE kinetics, according to the method described in [23], give the ZFS parameters, the relative populating rates and decay rates for the peridinin triplet sublevels in Chl *a* N-PCP and Chl *d* N-PCP reported in Table 1. Simulated DAF curves are shown in Fig. 3. As previously discussed [20–21], the ZFS axes correspond to those shown in the molecular structure of peridinin in Fig. 1. The order of the ZFS energy levels is: $Z^2 > Y^2 > X^2$. It can be seen that the ZFS parameters, the decay rates and the population probabilities, obtained from the simulation of the triplet spectra of Chl *a* N-PCP, are slightly different from those of native MFPCP. The introduction of Chl *d* in place of Chl *a* leads to a measurable effect on the relative population probabilities, but does not change the polarization pattern of the initial triplet spectrum (*eaeaea*), the ZFS parameters and the decay rates of the spin sublevels compared to Chl *a* N-PCP.

3.3. Triplet–triplet energy transfer

Calculations of the initial ESE triplet spectra based on the concept of spin conservation during the triplet-triplet energy transfer can be

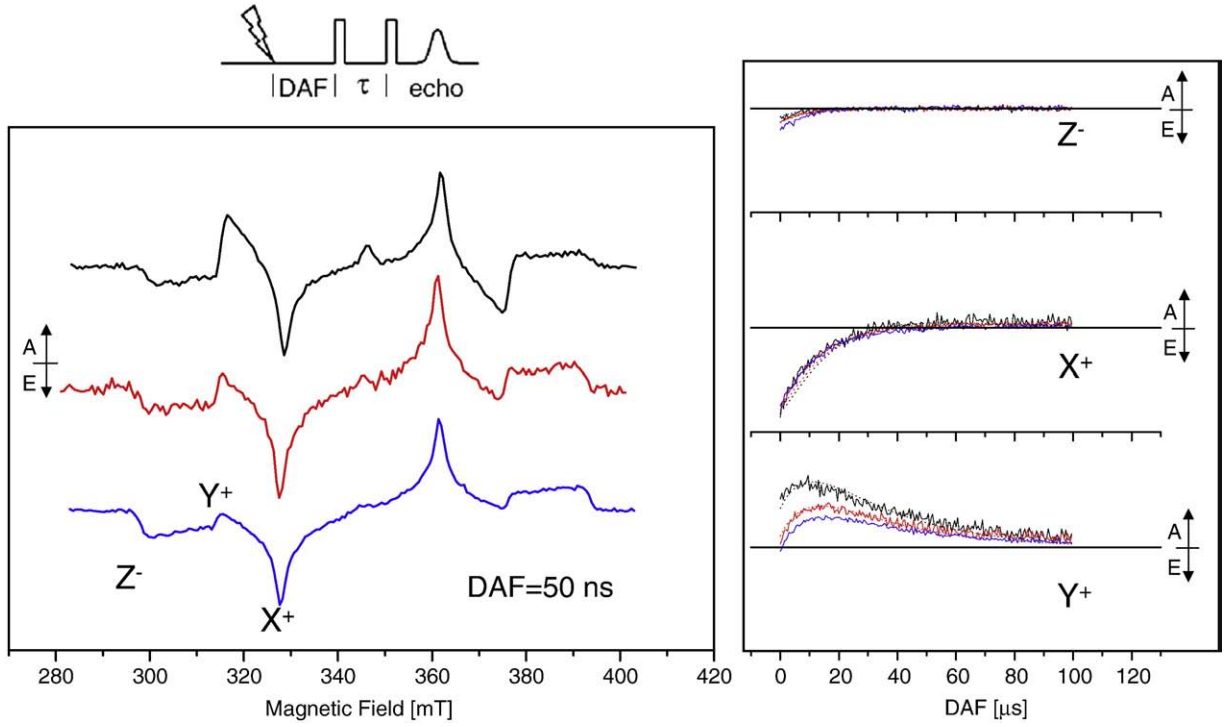

Fig. 3. (Left) Field-swept ESE spectrum of Chl *a* N-PCP (red), Chl *d* N-PCP (black) from *A. carterae*, at *T*=20 K, at DAF=50 ns. (Right) ESE-detected kinetics, at *T*=20 K, at the low-field canonical fields Z−, Y+, X+ (Chl *a* N-PCP (red), Chl *d* N-PCP (black)). A=absorption, E=emission. Simulated traces of Chl *a* N-PCP (red) and Chl *d* N-PCP (black) are superimposed on the experimental ones (dots). For experimental conditions see Section 2. Inset: Pulse scheme of the ESE experiment for photoexcited triplet states. Order of energy for zero field triplet sublevels: |Z|>|X|>|Y|. Data for MFPCP are from ref. [23].

performed by the method, previously described for native MFPCP [20,21]. Briefly, the acceptor (peridinin) inherits the spin polarization of the triplet donor in a way which depends on the relative geometrical arrangement of the donor-acceptor couple. Calculations for Chl *a* N-PCP have been performed assuming the same pigment arrangement of the N-domain of native MFPCP as derived from the X-ray structure, and initial Chl *a* spin level populations as those used for the calculations previously done on the native PCP [20]. The results (data not shown) inicate that in the reconstituted N-domain, the protein maintains the same characteristics of the triplet-triplet transfer as the full-length native protein, and the peridinins for which the calculations give a spectrum in agreement with the experimental one, are the same as in native PCP, namely PID614 and PID612 [20].

Calculations for Chl *d* N-PCP have been performed starting from a Chl *d* triplet state having the initial polarization pattern reported for isolated Chl *d* in 2-Me-THF glass: (Px:Py:Pz 0.34:0.50:0.16) [35]. The calculations assume the same relative geometry of the pigments as in the N-domain of MFPCP and in particular the same orientation of Chl *d* as Chl *a* in the binding pocket. The results are shown in Fig. 4 (left), where the spectra calculated for each Chl *d*→PID pair in the complex, are compared to the experimental spectrum. It can be seen that the best agreement with the experimental spectrum is achieved by assuming a localization of the triplet state on PID612. A good agreement with the experimental spectrum may be obtained also for PID 614 by rotating the ZFS axes of Chl *d* 15–20° around the axis perpendicular to the porphyrin plane (see Fig. 4, right). On the contrary the other two peridinins, PID611 and PID613, do not show the correct polarization pattern by small rotation of the ZFS axes (not shown).

4. Discussion

It is well established that triplet-triplet energy transfer, via the Dexter mechanism, is a process which depends strictly on the relative

Table 1
Parameters of the peridinin triplet state

	|D| (10^{-4} cm^{-1})	|E| (10^{-4} cm^{-1})	P_X: P_Y: P_Z	k_X: k_Y: k_Z (μs^{-1})	Ref
MFPCP	449.7±0.1 (ESE)	43.9±0.1 (ESE)	0.18:0.37:0.45	0.15: 0.03:0.09	[23]
	448.0±0.1 (ODMR)	44.0±0.1 (ODMR)			[18]
	458.6±0.1 (ODMR)	45.0±0.1 (ODMR)			[18]
Chl *a*	443.1±0.1 (ESE)	43.0±0.1 (ESE)	0.175:0.405:0.42	0.13: 0.034:0.09	
N-PCP					
	443.0±0.1 (ODMR)	43.0±0.5 (ODMR)			
Chl *d*	443.1±0.1 (ESE)	43.0±0.1 (ESE)	0.19: 0.435:0.375	0.13: 0.034:0.09	
N-PCP					
	443.0±0.1 (ODMR)	43.0±0.5 (ODMR)			

Values of the relative population rates, P_X, P_Y and P_Z, and decay constants, k_X, k_Y and k_Z, of the triplet sublevels in zero field together with the ZFS parameters |D| and |E|, derived from simulation of the time evolution of the field-swept ESE spectrum of Chl *a* N-PCP and Chl *d* N-PCP, according to the method described in ref [23]. For comparison the data relative to MFPCP from ref. [23] are also reported.
ZFS parameters resulting from the decomposition of the ODMR spectra of Chl *a* N-PCP and Chl *d* N-PCP with Gaussian components are also reported and compared to the equivalent data for MFPCP from ref. [18].

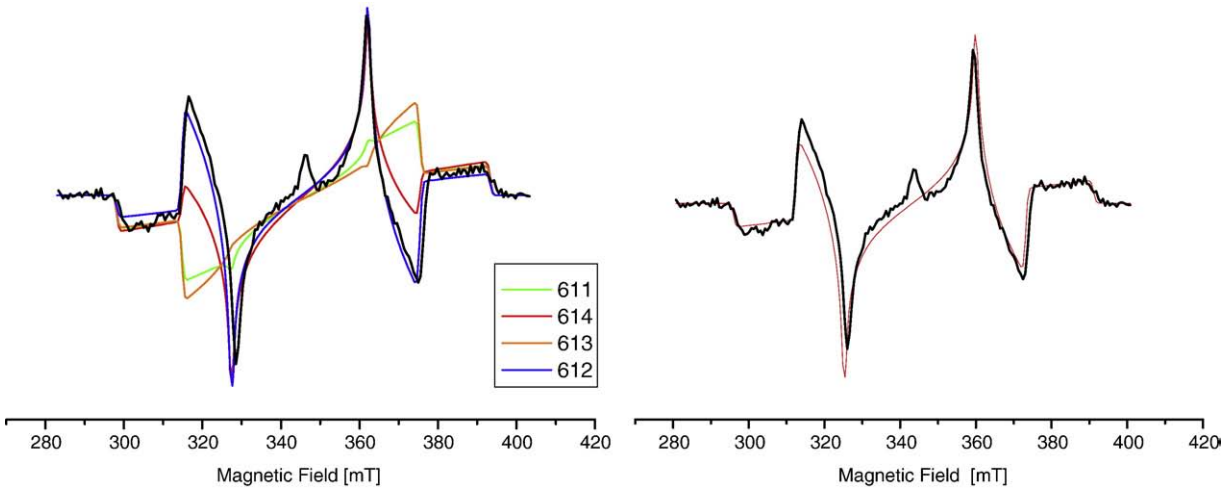

Fig. 4. (Left) Calculated initial triplet powder spectra of peridinins based on the triplet-triplet energy transfer mechanism, with the initial relative populations for the donor Chl *d* triplet: *Px:Py:Pz* = 0.34:0.50:0.16. Other parameters are reported in Table 1. The spectra are calculated for each Chl-Per pair of the N-domain as indicated. The spectra are compared to the experimental one, already reported in Fig. 3. (Right) Spectrum calculated for the Chl-PID614 pair after rotation (20°) of the ZFS axes of Chl *d* as discussed in the text.

geometry of donor and acceptor molecular frames. The efficiency of the photo-protection mechanism played by carotenoid molecules in the light harvesting complexes depends on the stringent overlap requirement between the chlorophyll and carotenoid wave functions. Any change in relative pigment geometry and/or in the electronic properties of the two partners in the triplet energy transfer may affect the efficiency of the process. In principle, by inserting Chl *d* in place of Chl *a* in N-PCP, some influence in the triplet-triplet transfer is expected, due to the different molecular structure (see Fig. 1) of the pigments.

4.1. ODMR

It is well kwon that the high sensitivity of the ODMR technique allows detection of very small amount of Chl triplet state. However no signals which could be ascribed to the presence of either Chl *a,* or Chl *d* triplet states have been detected in the N-PCP complexes. This means that the efficiency of triplet quenching is 100%, as in native PCP [21] and is not affected, either by the reconstitution process, or by the substitution of Chl *d* for Chl *a*.

The comparison of the T−S spectra of Chl *a* N-PCP and native MFPCP reported in Fig. 2 shows that the general features are maintained in the two complexes. The main T–T absorption band is centred at the same wavelength (567 nm) and the red-most bleaching in the peridinin absorption region is at ~535 nm in both complexes. However in Chl *a* N-PCP the main absorption band is less broad and more asymmetric. On the other hand, the T−S spectra of Chl *a* N-PCP and Chl *d* N-PCP are identical in the range from 450 to 650 nm. The ZFS parameters measured for the peridinin triplet state of Chl *a*-N-PCP and Chl *d* N-PCP differ less from each other than from those of native MFPCP. The small differences observed in the ZFS parameters and in the features of the carotenoid spectral region of the T−S spectra of the two N-PCP complexes compared to those of native MFPCP, could be due to the reconstitution process. Although the PCP complex reconstituted using the N-domain forms a dimer in solution, and aligning the duplicated N-domains on the published PCP structure, requires almost no spatial adjustment [36], the presence of only half protein may well introduce small changes in the molecular environment of the peridinins carrying the triplet states. In fact, looking closer at the interface between the two monomers, a deviation from a perfect matching is found, due to a relatively low identity between the N- and C-domains of MFPCP. The main deviations are in the loops surrounding the terminal ring close to the allene group of PID614/624 and where the tails of PID612/622 point toward the external solvent. Due to the length of the peridinins spanning the protein scaffold and to the close proximity of all the pigments in the two clusters, some effect could be transmitted to the whole interface producing a small structural rearrangement. This could influence the optical and magnetic properties of the peridinin carrying the triplet state as observed. The best overlay of the MFPCP structure with the dimer of two N-domains is shown in Supplementary material.

Significant differences in the T−S spectra of Chl *a* N-PCP and Chl *d* N-PCP, are present only in the region of the Qy absorption bands of the Chls. As expected the bleaching of Chl *d* is red-shifted compared to Chl *a* and is centered at 695 nm. If the T−S spectra of Chl *a* N-PCP and Chl *d* N-PCP are normalized at 570 nm, the intensity of the Q_y bleaching is 1.5 times greater for Chl *a* compared to Chl *d*. Since the extinction coefficient is about the same, or even higher, for Chl *d* in PCP [4] the difference can be ascribed to a different interaction strength between the Chl (*a* or *d*) and the peridinin carrying the triplet state, as proposed by Angerhofer et al. [37] to explain the results on triplet-triplet transfer efficiency in bacterial light harvesting complexes.

It is interesting to note that the up to now unassigned triplet–triplet absorption bands, appearing between 580–660 nm in the T−S spectra, must belong to the peridinin triplet manifold since they are not influenced by the change in electronic properties following substitution of Chl *a* by Chl *d*.

4.2. Pulse EPR and triplet–triplet transfer

The presence of only minor differences in the ESE (or in the TR-EPR) spectra taken at initial times after the laser flash and in the kinetics of Chl *a* N-PCP compared to those of native MFPCP, indicates that the peridinins responsible for the Chl triplet quenching are substantially unaltered, in terms of their relative orientation with respect to the ^{T}Chl donor, and in terms of their ZFS axes in the peridinin manifold. The minor differences observed may be due to the interface effects mentioned above in discussing the ODMR results.

Calculations of the initial polarization of the ESE spectra in Chl *a* N-PCP, based on the assumption of spin conservation during triplet-triplet energy transfer, show that the best agreement with the experimental data is achieved, as in native MFPCP, by localising the triplet on PID614 and, possibly, in PID612. In the case of native MFPCP significant contribution of PID612 was considered to be unlikely, based on comparison with HSPCP which shows similar initial polarization of the ESE spectra but lacks PID612 although maintaining a similar pigment arrangement [21]. The same consideration can be extended to Chl *a* N-PCP.

The comparison between the relative populations of the peridinin triplet spin sublevels of Chl *d* N-PCP and Chl *a* N-PCP, show that the introduction of Chl *d*, leads to a significant change of the initial population probabilities, while the ZFS parameters and the decay rates are conserved. The calculations of the initial ESE spectra reported in Fig. 4, for Chl *d* N-PCP seem to indicate a preferential quenching by PID612 compared to PID614, while the other two peridinins (PID611-613) are characterized by a wrong polarization pattern and their contribution must be negligible. This result is however surprising because PID612 is postulated to be a blue-shifted peridinin, absorbing at ~485 nm in native MFPCP. If high energy absorption is maintained in the N-PCP reconstituted domain, a preferential localization of the triplet state on the blue-absorbing peridinin would produce a large effect on the associated T−S spectrum. The main bleaching should be blue-shifted and the T–T absorption band would be expected at shorter wavelengths. On the contrary the T−S spectrum of the Chl *d* N-PCP is almost identical to that of Chl *a* N-PCP and similar to that of native PCP in the peridinin absorption region. According to Ilagan et al. [4] the 10 K absorption spectrum of Chl *d* N-PCP results from contribution of four spectrally distinct forms of peridinin with spectral origins at 490, 513, 530, 546 nm, substantially the same as in Chl *a* N-PCP (486, 510, 529, 548 nm) and very similar to those of the native PCP (485, 522, 526, 544 nm). If the localization of the triplet state changed upon reconstitution with Chl *d*, large effects on the T−S spectrum would be expected, but this is not observed. The ODMR data clearly indicate no changes in terms of magnetic and optical properties of the peridinin(s) triplet state(s) involved in the Chl triplet quenching. Furthermore the decay rates of spin sublevels, determined by the simulations of ESE spectra, are the same as those found for Chl *a* N-PCP (Table 1).

As mentioned above, the calculation of triplet–triplet energy transfer in Chl *d* N-PCP, is based on the assumptions of an initial Chl *d* triplet state having the polarization pattern reported for isolated Chl *d* in 2-MTHF glass (Px:Py:Pz 0.34:0.50:0.16) [33], the same ZFS axes directions as for Chl *a*, the same relative geometry of the pigments as in the N-domain of the native MFPCP and in particular the same orientation of Chl *d* in the binding pocket of Chl *a*. The effect of the polarization of Chl *d* triplet donor has been checked by determining the population probabilities of Chl *d* in partially denatured samples of Chl *d* N-PCP where the Chl *d* triplet state becomes detectable due to reduced triplet-triplet energy transfer efficiency. This experiment gives the following parameters: Px:Py:Pz 0.33:0.43:0.24 for Chl *d*. Using this different set of initial Chl triplet state populations does not change the results significantly, meaning that the best agreement between the experimental and calculated triplet spectra is still reached by localising the triplet preferentially on PID612 (data not shown). This makes the choice of the Chl *d* initial population probabilities, within the range of population above mentioned, not crucial for the assignment of the peridinin involved in the triplet energy transfer. Out of the range the agreement becomes poor for small changes of the Pz population, while the Px and Py values are less restrictive. Instead, a change of the ZFS axes directions in the Chl molecular structure, or a rotation of the Chl ring in the protein, could both account for the observed effects. In fact, when we calculate the acceptor spectrum by rotating the ZFS axes of Chl *d* 15–20° around the axis perpendicular to the porphyrin plane, we obtain a good agreement, with the experimental spectrum, for PID 614 (see Fig. 4). In principle, a change of the axes directions with respect to Chl *a*, due to the substitution in ring 1 (R1) of the porphyrin, is possible. Unfortunately, the directions of the ZFS axes in Chl *d* have not yet been determined either in vitro or in vivo. This leaves open the other possibility for the interpretation of the data: the results are still compatible with a localization of the triplet state on PID614, as in native PCP, if, instead of rotating the ZFS axes in the molecular plane, a rotation of the Chl *d* ring takes place, when the pigment is placed in the binding pocket of Chl *a*. It is interesting to note that such a rotation could be accompanied by the formation of a H-bond of the carbonyl group with the -OH group of the terminal ring of PID612 (see Supplementary material for details). This pigment rearrangement would also be in agreement with the ODMR measurements showing a small change of Chl-peridinin interaction, as revealed by the different intensity of the Q_y bleaching in T−S spectra of Chl *a* N-PCP and Chl *d* N-PCP. A local effect in the binding of Chl *d* in PCP has been invoked also by Ilagan et al. [4] who suggested that the carbonyl group of Chl *d* in R1 unlike the vinyl group of Chl *a* (see Fig. 1) is unable to assume different conformations, explaining in this way the lack of splitting of the Chl Soret band on binding Chl *d* into PCP.

In our previous work on MFPCP and HSPCP we have suggested that the water molecule coordinated to the central Mg of the Chl molecules, plays a key role in the triplet-triplet transfer in MFPCP, and in HSPCP, by forming a bridge between the Chl and PID614/624 (PID1331/1335 in HSPCP) [21]. Since the rotation of Chl *d* does not preclude the possibility of forming a water bridge between Chl *d* and PID614 in N-PCP, the localization of the triplet state on PID614 could still predominate.

5. Conclusions

The N-PCP complexes maintain a 100% efficiency for the quenching of chlorophyll despite the biochemical treatment and reconstitution process, suggesting a substantially conserved pigment structure and arrangement, compared to the native MFPCP. Analysis of the T−S spectra, initial polarization of the photoinduced field-swept ESE spectra and their time evolution, show that, in the reconstituted complexes, the triplet state is probably localized on the same peridinin as in the native complex, although, when Chl *d* replaces Chl *a* in the binding pocket, a local rearrangement of the pigments could occur.

Acknowledgements

This work was supported by the Italian Ministry for University and Research (MURST) under the project PRIN2005. We are grateful to Prof. Giovanni Giacometti for his continuous interest in this work.

Appendix A. Supplementary data

Supplementary data associated with this article can be found, in the online version, at doi:10.1016/j.bbabio.2008.12.004.

References

[1] A. Macpherson, R.G. Hiller, Light-harvesting system in Chl *c*-containing algae in: light-harvesting antennas, in: B Green, W Parson (Eds.), Photosynthesis, Kluwer, Dordrecht, 2003, pp. 323–352.
[2] E. Hofmann, P.M. Wrench, F.P. Sharples, R.G. Hiller, W. Welte, K. Diederichs, Structural basis of light harvesting by carotenoids: Peridinin-chlorophyll-protein from *Amphidinium carterae*, Science 272 (1996) 1788–1791.
[3] F.P. Sharples, P.M. Wrench, K.L. Ou, R.G. Hiller, Two distinct forms of the peridinin-chlorophyll a-protein from Amphidinium carterae, Biochim. Biophys. Acta 1276 (1996) 117–123.
[4] R.P. Ilagan, T.W. Chapp, R.G. Hiller, F.P. Sharples, T. Polívka, H.A. Frank, Optical spectroscopic studies of light-harvesting by pigment-reconstituted peridinin-chlorophyll-proteins at cryogenic temperatures, Photosynth. Res. 90 (2006) 5–15.
[5] R.P. Ilagan, S. Shima, A. Melkozernov, S. Lin, R.E. Blankenship, F.P. Sharples, R.G. Hiller, R.R. Birge, H.A. Frank, Spectroscopic properties of the main-form and high-salt peridinin-chlorophyll a proteins from *Amphidinium carterae*, Biochemistry 43 (2004) 1478–1487.
[6] F.J. Kleima, M. Wendling, E. Hofmann, E.J.G. Peterman, R. van Grondelle, H. van Amerongen, Peridinin chlorophyll a protein: relating structure and steady-state spectroscopy, Biochemistry 39 (2000) 5184–5195.
[7] D. Carbonera, G. Giacometti, U. Segre, E. Hofmann, R.G. Hiller, Structure-based calculations of the optical spectra of the light-harvesting peridinin-chlorophyll-protein complexes from *Amphidinium carterae* and *Heterocapsa pygmaea*, J. Phys. Chem., B 103 (1999) 6349–6356.
[8] E. Papagiannakis, M. Vengris, D.S. Larsen, I.H.M. van Stokkum, R.G. Hiller, R. van Grondelle, Use of ultrafast dispersed pump-dump-probe and pump-repump-probe spectroscopies to explore the light-induced dynamics of peridinin in solution, J. Phys. Chem., B 110 (2006) 512–521.

[9] A. Damjanovic, T. Ritz, K. Schulten, Excitation transfer in the peridinin-chlorophyll-protein of *Amphidinium carterae*, Biophys. J. 79 (2000) 1695–1705.
[10] D.J. Miller, J. Catmull, R. Puskeiler, H. Tweedale, F.P. Sharples, R.G. Hiller, Reconstitution of the peridinin-chlorophyll *a*-protein (PCP): evidence for functional flexibility in chlorophyll binding, Photosynth. Res. 86 (2005) 229–240.
[11] T.H.P. Brotosudarmo, H. Hofmann, R.G. Hiller, S. Wörmke, S. Mackowski, A. Zumbusch, C. Bräuchle, H. Scheer, Peridinin-chlorophyll-protein reconstituted with chlorophyll mixtures: preparation, bulk and single molecule spectroscopy, FEBS Lett. 580 (2006) 5257–5262.
[12] T.H.P. Brotosudarmo, S. Mackowski, E. Hofmann, R.G. Hiller, C. Bräuchle, H. Scheer, Relative binding affinities of chlorophylls in peridinin-chlorophyll-protein reconstituted with heterochlorophyllous mixtures, Photosynth. Res. 94 (2008) 247–252.
[13] T. Polivka, T. Pascher, V. Sundstrom, R.G. Hiller, Tuning energy transfer in the peridinin-chlorophyll complex by reconstitution with different chlorophylls, Photosynth. Res. 86 (2005) 217–227.
[14] T. Polivka, T. Pascher, R.G. Hiller, Energy transfer in the peridinin-chlorophyll protein complex reconstituted with mixed chlorophyll sites, Biophys. J. 94 (2008) 3198–3207.
[15] S. Mackowski, S. Wörmke, T.H.P. Brotosudarmo, C. Jung, R.G. Hiller, H. Scheer, C. Bräuchle, Energy transfer in reconstituted peridinin-chlorophyll-protein complexes: ensemble and single molecule spectroscopy studies, Biophys. J. 93 (2007) 3249–3258.
[16] S. Mackowski, S. Wörmke, T.H.P. Brotosudarmo, H. Scheer, C. Bräuchle, Fluorescence spectroscopy of reconstituted peridinin-chlorophyll-protein complexes, Photosynth. Res. 95 (2008) 253–260.
[17] H.A. Frank, R.J. Cogdell, Carotenoids in photosynthesis, Photochem. Photobiol. 63 (1996) 257–264.
[18] D. Carbonera, G. Giacometti, G. Agostini, FDMR spectroscopy of peridinin chlorophyll-a protein from amphidinium-carterae, Spectrochimica 51A (1995) 115–123.
[19] J.A. Bautista, R.G. Hiller, F.P. Sharples, D. Gosztola, M. Wasielewski, H.A. Frank, Singlet and triplet energy transfer in the peridinin-chlorophyll a-protein from *Amphidinium carterae*, J. Phys. Chem., A 103 (1999) 2267–2273.
[20] M. Di Valentin, S. Ceola, E. Salvadori, G. Agostini, D. Carbonera, Identification by time-resolved EPR of the peridinins directly involved in chlorophyll triplet quenching in the peridinin-chlorophyll a-protein from *Amphidinium carterae*, Biochim. Biophys. Acta 1777 (2008) 186–195.
[21] M. Di Valentin, S. Ceola, E.o. Salvadori, G. Agostini, G.M. Giacometti, D. Carbonera, Spectroscopic properties of the peridinins involved in chlorophyll triplet quenching in high-salt peridinin-chlorophyll a-protein from Amphidinium carterae as revealed by optically detected magnetic resonance, pulse EPR and pulse ENDOR spectroscopies, Biochim. Biophys. Acta 1777 (2008) 1355–1363.
[22] J. Niklas, T. Schulte, S. Prakash, M. van Gastel, E. Hofmann, W. Lubitz, W. Spin, Density distribution of the carotenoid triplet state in the peridinin-chlorophyll-protein antenna. A Q-band pulse electron-nuclear double resonance and density functional theory study, J. Am. Chem. Soc. 129 (2007) 15442–15443.
[23] M. Di Valentin, S. Ceola, G. Agostini, G.M. Giacometti, A. Angerhofer, O. Crescenzi, V. Barone, D. Carbonera, Pulse ENDOR and density functional theory on the peridinin triplet state involved in the photo-protective mechanism in the peridinin-chlorophyll a-protein from Amphidinium carterae, Biochim. Biophys. Acta 1777 (2008) 295–307.
[24] R.H. Clarke, Triplet state ODMR spectroscopy, in: R.H. Clarke (Ed.), Techniques and Applications to Biophysical Systems, Wiley-Interscience, New York, 1982.
[25] A.J. Hoff, Optically detected magnetic resonance of triplet states, in: A.J. Hoff (Ed.), Advanced EPR, Elsevier, Amsterdam, 1989.
[26] T.A. Martinson, G.F. Plumley, One-step extraction and concentration of pigments and acyl lipids by *sec*-butanol from *in vitro* and *in vivo* samples, Anal. Biochem. 228 (1995) 123–130.
[27] D. Carbonera, G. Giacometti, G. Agostini, FDMR of carotenoid and chlorophyll triplets in Light-harvesting complex LHCII of spinach, Appl. Magn. Reson. 3 (1992) 361.
[28] S. Santabarbara, E. Bordignon, R.C. Jennings, D. Carbonera, Chlorophyll triplet states associated with photosystem II of thylakoids, Biochemistry 41 (2002) 8184.
[29] S. Stoll, A. Schweiger, EasySpin, a comprehensive software package for spectral simulation and analysis in EPR, J. Magn. Reson. 178 (2006) 42–55.
[30] D. Carbonera, G. Giacometti, G. Agostini, A. Angerhofer, V. Aust, ODMR of carotenoid and chlorophyll triplets in CP43 and CP47 complexes of spinach, Chem. Phys. Lett. 194 (1992) 275–281.
[31] D. Carbonera, E. Bordignon, G. Giacometti, G. Agostini, A. Vianelli, Fluorescence and absorption detected magnetic resonance of chlorosomes from green bacteria Chlorobium tepidum and *Chloroflexus aurantiacus*. A comparative study, J. Phys. Chem., B 105 (2001) 246–255.
[32] D. Carbonera, G. Agostini, T. Morosinotto, R. Bassi, Quenching of chlorophyll triplet states by carotenoids in reconstituted Lhca4 subunit of peripheral light-harvesting complex of photosystem I, Biochemistry 44 (2005) 8337–8346.
[33] D. Carbonera, G. Giacometti, U. Segre, A. Angerhofer, U. Gross, Model for triplet-triplet energy transfer in natural clusters of peridinin molecules contained in Dinoflagellate's outer antenna proteins, J. Phys. Chem., B 103 (1999) 6357–6362.
[34] D. Carbonera, G. Giacometti, U. Segre, Carotenoid interactions in peridinin chlorophyll a proteins from dinoflagellates — evidence for optical excitons and triplet migration, J. Chem. Soc., Faraday Trans. 92 (1996) 989–993.
[35] M. Di Valentin, S. Ceola, G. Agostini, A. Telfer, J. Barber, F. Böhles, S. Santabarbara, D. Carbonera, The photo-excited triplet state of chlorophyll *d* in methyl-tetrahydrofuran studied by optically detected magnetic resonance and time-resolved EPR, Mol. Phys. 105 (2007) 2109–2117.
[36] R.G. Hiller, L.G. Crossley, P.M. Wrench, N. Santucci, E. Hofmann, The 15-kDa forms of apo-peridinin-chlorophyll *a* protein (PCP) in dinoflagellates show high identity with the apo-32-kDa PCP forms, and have similar N-terminal leaders and gene arrangements, Gent. Genomics 266 (2001) 254–259.
[37] A. Angerhofer, F. Bornhauser, A. Gall, R.J. Cogdell, Optical and optically detected magnetic resonance investigation on purple photosynthetic bacterial antenna complexes, Chem. Phys. 194 (1995) 259–274.